Title: Characterizing biofilm interactions between *Ralstonia insidiosa* and *Chryseobacterium gleum*

Running title: *Ralstonia-Chryseobacterium* biofilm interactions

Andrea Foote[a], Kristin Schutz[b], Zirui Zhao[c], Pauline DiGianivittorio[a,b], Bethany R. Korwin-Mihavics [a], John J. LiPuma[d], and Matthew J. Wargo[b,#]

[a] Cellular, Molecular, and Biomedical Sciences Graduate Program, and [b] Department of Microbiology and Molecular Genetics, University of Vermont Larner College of Medicine, Burlington, Vermont, USA

[c] Department of Biology, University of Vermont, Burlington, Vermont, USA

[d] Department of Pediatrics, University of Michigan Medical School, Ann Arbor, Michigan, USA.

Corresponding author

Matthew J. Wargo

95 Carrigan Drive, 308 Stafford Hall, Burlington, VT 05405

mwargo@uvm.edu

P: 802-656-1115

Key Words: tap water microbiology, bacterial ecology, dual-species biofilms, bacterial interactions

Abstract

Ralstonia insidiosa and *Chryseobacterium gleum* are bacterial species commonly found in potable water systems and these two species contribute to the robustness of biofilm formation in a model six-species community from the International Space Station (ISS) potable water system. Here, we set about characterizing the interaction between these two ISS-derived strains and examining the extent to which this interaction extends to other strains and species in these two genera. The enhanced biofilm formation between the ISS strains of *R. insidiosa* and *C. gleum* is robust to starting inoculum and temperature, occurs in some but not all tested growth media, and evidence does not support a soluble mediator or co-aggregation mechanism. These findings shed light on the ISS *R. insidiosa* and *C. gleum* interaction, though such enhancement is not common between these species based on our examination of other *R. insidiosa* and *C. gleum* strains, as well as other species of Ralstonia and Chryseobacterium. Thus, while the findings presented here increase our understanding of the ISS potable water model system, not all our findings are broadly extrapolatable to strains found outside of the ISS.

Importance:

Biofilms present in drinking water systems and terminal fixtures are important for human health, pipe corrosion, and water taste. Here we examine the enhanced biofilm of cu-cultures for two very common bacteria from potable water systems, *Ralstonia insidiosa* and *Chryseobacterium gleum*. While strains originally isolated on the International Space Station show enhanced dual-species biofilm formation, terrestrial strains do not show the

same interaction properties. This study contributes to our understanding of these two species in both dual and mono-culture biofilm formation.

Introduction

Multispecies, surface-attached biofilms are an important part of the built environment, particularly the potable water system that includes the municipal delivery system, building plumbing, terminal fixtures, appliances, and associated surfaces [1-6]. Potable water system biofilms contribute to alterations in material corrosion, water properties, and health of those drinking and bathing in the water [7]. While the microbial communities within these systems are diverse, there are a number of taxa that are common across wide swaths of geography and water chemistry, including the genera *Ralstonia* and *Chryseobacterium* [8]. *Ralstonia insidiosa* and its close relative, *Ralstonia pickettii*, are beta proteobacteria that are common in water systems and other parts of the built environment [9, 10] and can be found infrequently as opportunistic pathogens in human infections [11-14]. *Chryseobacterium gleum* (formerly, *Flavobacterium gleum*) in the phylum Bacteroidetes, is present in similar environments as *R. insidiosa* and can also be present in human infections [15-17], though less frequently.

R. insidiosa promotes biofilms in conjunction with a number of species including *Listeria monocytogenes*, *Salmonella enterica*, and *Escherichia coli* [18-22]. In most of these cases, *R. insidiosa* has been reported as a physical bridge between cells of the other species with components of the biofilm matrix predicted as driving the enhanced biofilms [21, 22]. *Chryseobacterium* species are reported as strong biofilm formers in

single-species cultures [17], but their enhancement of multispecies biofilms has not been reported as frequently [23].

We previously reported that strains of *R. insidiosa* isolate and *C. gleum* from the International Space Station (ISS) were capable of enhanced dual-species biofilm formation, though neither was capable of robust biofilm formation alone [24]. This interaction is a critical facet for robustness of biofilm formation in this six-species model drinking water community [24]. Here we characterize the interaction between *R. insidiosa* and *C. gleum* in relation to biofilm formation, examining potential broad mechanisms, the dependence of the interaction on growth conditions, and the broader applicability of this interaction by testing other strains and species within these two genera.

Methods

Bacterial strains and maintenance conditions

R. insidiosa 130770013-1 was isolated from the ISS Potable Water Delivery System and *C. gleum* 113330055-2 was isolated from the Russian SVO-ZV module on the ISS, and both identified by the Microbiology Laboratory at the NASA Johnson Space Center (Houston, TX) [1]. The strain numbers listed after each species are for the strain database at the Johnson Space Center, and strains may be requested directly using these designations. Terrestrial strains of *R. insidiosa*, *R. pickettii*, *C. gleum*, *Chryseobacterium indologenes*, *Chryseobacterium meningosepticum*, and *Ralstonia* strains that cannot be identified as belonging to one of the currently named species in this genus were acquired from the Cystic Fibrosis Foundation *Burkholderia cepacia* Research Laboratory and Repository at the University of Michigan. Details on all strains presented

in **Table 1**. All bacteria were stored in 20% glycerol stocks at -80°C and were recovered on R2A plates at 30°C.

For all experiments below, the R2A plates were used as a source of inoculation into MRLP media [24] (2/3rd modified MOPS media [25], 1/3rd R2B, with 2% LB and 10 mM sodium pyruvate; in composition, this medium comprises 26.4 mM MOPS, 2.64 mM tricine, 6.28 mM NH_4Cl, 34.7 mM NaCl, 0.35 mM $MgCl_2$, 0.19 mM K_2SO_4, 1.57 mM K_2HPO_4, 10.91 mM sodium pyruvate, 0.94 mM glucose, 32 µM $MgSO_4$, 21.1 µM $CaCl_2$, 6 µM $FeSO_4$, 5.28 µM $FeCl_2$, 0.33 g l^{-1} peptone, 0.27 g l^{-1} yeast extract, 0.20 g l^{-1} tryptone, 0.17 g l^{-1} soluble starch, and 0.66X MOPS medium micronutrients) and cells were grown overnight in 3 ml culture volume at 30°C with orbital shaking of angled, loosely capped 18 x 150 mm glass tubes. Some experiments were also conducted in a high calcium version of MRLP where the final $CaCl_2$ concentration was 400 µM. The higher calcium concentration increases monoculture biofilm formation for *C. gleum* as described in the results section, but co-culture enhancement is still apparent. Calcium concentration is noted in each figure legend.

Other media formulations were also tested to assess the range of conditions within which coculture biofilm enhancement could be seen. These included versions of MRLP where the 2/3 volume of minimal media was switched from MOPS to M9 or M63 to generate M9-RLP and M63-RLP, respectively. Additionally, RL media was used which was 1/3 R2B with 2% LB with the remainder of the volume made up from distilled-deionized water.

<u>Biofilm initiation, quantification, and cell numbers</u>

For 96-well format static biofilms, overnight MRLP-grown cultures were used as the starting source for biofilm experiments. The optical density of each species was determined and normalized to generate an initial OD_{600} of 0.05 for each species member in MRLP. After pipetting 150 µl of the species mixtures into flexible 96-well plates, the plates were placed into humidified chambers and incubated under static conditions (no shaking) at 30 °C for 24 hours. To measure biofilm formation, the crystal violet staining protocol was used as described by O'Toole and colleagues [26]. Biofilms were quantified by dissolving the crystal violet with 10% acetic acid and measuring absorbance at 550 nm.

For rotating wall vessel (RWV) biofilms, cells were grown overnight as for the 96-well biofilms and then inoculated into 10 ml RWVs (Synthecon Inc., ethanol-sterilized and dried) at a starting inoculum of 0.008 OD_{600} per species. RWVs were rotated in the vertical orientation at room temperature overnight. In conducting the RWV experiments, we observed that most of the biomass, particularly in the dual-species culture, was present as a biofilm on the air-permeable membrane of the vessel. To measure these biofilms, the membrane was rinsed with sterile media and then scraped with a silicon cell scraper into a Petri dish containing additional sterile media. The contents of the Petri dish were then collected by centrifugation and pellets stained with crystal violet as above. After staining, pellets were washed twice before dissolution of the crystal violet in 10% acetic acid. Due to the large quantity of biofilm material, the crystal violet was quantified by two-fold serial dilutions, which were then corrected to total absorbance by multiplication with the respective serial dilution factor.

For biofilms on glass coverslips, 22 mm square coverslips were sterilized in ethanol and dried prior to insertion into 12-well plates. The coverslips fit snugly in the wells but rest slightly off of vertical. Each well contained 2.2 ml of high calcium MRLP, which was enough to reach about halfway up the coverslip. After inoculation as described for the 96-well biofilms, the 12-well dished were incubated statically at 30ºC in a humidified chamber for 20-24 hours.

To determine total cell number in the static 96-well plates (planktonic + biofilm), cells were gathered by resuspending the contents of each well via vigorous pipetting and scraping the well walls with a pipette tip. As measured by crystal violet staining, < 1% of the biomass remained after this treatment. The scraped well contents were vortexed to resuspend and serially diluted in R2B before plating onto R2A. For wells with both species, CFU counts for each species were determined by the obvious colony color difference (orange-yellow for *C. gleum*, and white/beige for *R. insidiosa*).

Statistical analysis and data visualization

All data visualization and statistical analyses were conducted in GraphPad Prism v9 using one-way or two-way ANOVA with Tukey, Sidak, Bonferroni, or Dunnett's post-testing as described in individual figures. Values of p below 0.05 were considered statistically significant. Data is presented, when possible, with bars representing the mean and either biological replicates or all experimental replicates shown as individual data point overlain. Even when all experimental replicates are depicted, statistical analysis is conducted using the means of each biological replicate only. Where individual data points

are not shown for clarity and figure size considerations, error bars represent standard deviation.

Generation of mScarlet-expressing *R. insidiosa*

We used *attTn7*-based chromosomal integration to generate stable fluorescent *R. insidiosa* using the general method for Gram-negative bacteria [27]. Briefly, we mixed *R. insidiosa* with *E. coli* S17-1 carrying pMRE-Tn7-145 [27] and allowed conjugation to occur on an LB plate with 0.1% L-arabinose overnight. The spot was scraped, resuspended, and *R. insidiosa* carrying the *attTn7* insertion were selected by plating on MOPS agar with 25 mM pyruvate, 10 mM glucose, 25 µg/ml gentamicin, and 10 µg/ml chloramphenicol. Colonies were picked and screened for presence of the *R. insidiosa* specific PCR product [11], the integration cassette via PCR for the gentamicin resistance gene (GmR-check-F 5'- TCTTCCCGTATGCCCAACTT-3' and GmR-check-R 5'-ACCTACTCCCAACATCAGCC-3'), and fluorescence concordant with mScarlet (using 565 excitation and 600 emission using a Biotek H1 multimode plate reader).

Microscopy

Fluorescence microscopy was carried out on a Nikon A1R-ER confocal laser microscope housed in the UVM Microscopy Imaging Center using the RFP laser and emission filter for mScarlet which, while not optimized for mScarlet, still allowed visualization of the mScarlet signal. Images were captured and analyzed with Nikon NIS-Elements software.

Results

Co-culture of the ISS *Chryseobacterium gleum* and *Ralstonia insidiosa* leads to enhanced biofilm formation

We had previously observed that the ISS isolates of *R. insidiosa* and *C. gleum* in our six-member potable water biofilm community demonstrated enhanced biofilm formation together and very little when grown alone [24]. The goal of this project was to extend the characterization of this interaction. Partly to aid in this endeavor, we generated a clone of the ISS *R. insidiosa* carrying mScarlet at the *attTn7* site. Both the parent strain of *R. insidiosa* and the *R. insidiosa* with mScarlet showed enhanced biofilm formation with *C. gleum* in flexible 96-well dish biofilms (**Figure 1A**). This enhanced biofilm formation is not due solely to growth stimulation of either species during co-culture (**Figure 1B**).

To examine the enhanced biofilm microscopically, we grew each biofilm on glass coverslips positioned roughly vertically in 12-well dishes. To visually assess biofilm formation, we stained duplicate coverslips with crystal violet. Enhanced biofilm is apparent in the co-cultures, and we also note that *R. insidiosa attTn7::mScarlet* forms a stronger mono-culture biofilm on glass than it does on plastic (**Figure 2A**), which is not different than the untagged *R. insidiosa* on glass. The doublet line, most apparent in the co-culture, is formed because the coverslip rests at an angle off vertical; the surface film intercepts at slightly different positions on each side of the coverslip. For fluorescent microscopy, we wiped one side thoroughly with paper cloth after fixation to remove material from the side not being viewed. Imaging of the co-culture biofilm showed red-fluorescent cells that were co-stained with DAPI (*R. insidiosa*), as well as cells fluorescing

205 solely with DAPI (*C. gleum*) (**Figure 2B**). Like other examples of *R. insidiosa* enhancing
206 biofilm formation [19-22], this dual-species biofilm is intermixed.
207
208 The impact of calcium concentration on *C. gleum* biofilm formation
209 During compilation of the data and final sets of experimentation, it was noticed that
210 while enhanced biofilm was always obvious between these two strains of bacteria, the
211 baseline biofilm formation by *C. gleum* was very different between different experimenters
212 and compared to our previous work [24]. A deep dive through lab notebooks uncovered
213 the likely difference as two different recipes for our MRLP media in the lab that differed
214 only in their final calcium concentrations: 21.1 µM vs 400 µM. To test whether this calcium
215 difference was able to explain the *C. gleum* biofilm differences between experimenters,
216 we tested freshly made versions of both MOPS recipes. High calcium increases *C. gleum*
217 biofilm formation (**Figure 3**). There is roughly 5-fold higher biofilm formation by *C. gleum*
218 grown in high calcium versus in low calcium. The dual-species biofilms were also
219 enhanced by high calcium growth, but biofilm for *R. insidiosa* remained unchanged.
220 Because we saw enhanced biofilm at either calcium level, we present data from both
221 calcium conditions in this paper and note the calcium level in the figure legends.
222
223 The biofilm stimulation between these strains is robust to starting inoculum
224 Our initial studies used equal starting OD's for each species and we chose to next
225 examine the robustness of the enhanced biofilm formation to starting inoculum. If we
226 changed the ratio of the starting inoculum of *C. gleum* to *R. insidiosa* from 10% *C. gleum*
227 (90% *R. insidiosa*) to 90% *C. gleum* (10% *R. insidiosa*), where 50% *C. gleum* is our

228 previously reported 1:1 mixture, we saw that all combinations resulted in enhanced biofilm
229 formation compared to *C. gleum* alone (100% *C. gleum*), particularly at the lower
230 proportions of *C. gleum* (**Figure 4A**). Further dilution of *C. gleum* compared to a set
231 proportion of *R. insidiosa* showed that some biofilm enhancement of the co-culture
232 compared to that of *R. insidiosa* alone was retained down to 0.0001% *C. gleum* (roughly
233 15 *C. gleum* cells per well at time of inoculation) (**Figure 4B**).
234
235 Media and environmental impacts on the *C. gleum/R. insidiosa* interaction
236 After observing that the enhanced biofilm formation in the *C. gleum*/*R. indiosa* co-
237 culture was very robust to the starting inoculum (**Fig. 4**) and that calcium concentration
238 could alter *C. gleum* mono- and co-culture biofilm formation (**Fig. 3**), we expanded the
239 parameters and examined the impacts of media composition, temperature, and low-shear
240 simulated microgravity conditions.
241 In an initial attempt to simplify the media composition, replacement of the MOPS
242 media in our standard MRLP with M9 (M9-RLP) or M63 (M63-RLP) was attempted, as
243 was the RL composition (see Materials & Methods for precise descriptions). When
244 overnight cultures were pre-grown in MRLP and used to inoculate biofilm formation in
245 various media, all tested media supported some level of enhanced biofilm between *R.*
246 *insidiosa* and *C. gleum* (**Figure 5A**). However, when overnights were pre-grown in M9-
247 RLP, biofilm enhancement was only seen in MRLP and RL media, while no significant
248 biofilm enhancement was seen with M9-RLP or M63-RLP (**Figure 5B**). In data not shown
249 here, pre-growth in RL media was similar to MRLP, while pre-growth in M63-MRLP was
250 similar to M9-RLP. One of the primary differences between MRLP/RL vs M9-RLP/M63-

RLP is phosphate concentration, but we have not formally tested if phosphate is the contributing factor in these media differences.

We also tested whether enhanced biofilm formation by *C. gleum* and *R. insidiosa* was achieved at higher temperatures. Both species are opportunistic pathogens and thus capable of growth at body temperature. When grown at 37ºC, similar biofilm enhancement between these species was observed as when grown at 30ºC (**Figure 5C**).

Finally, the focus of these studies were two strains collected from the ISS and thus previously subjected to continuous microgravity and the low-shear environment that accompanies such gravity conditions. To mimic the low-shear component of microgravity, we used rotating wall vessels (RWVs) where the cells in suspension have defined vertical circular paths within a low-shear environment. While some clumping was seen for the cells in suspension in the dual-species RWV cultures, we noted that most of the biomass was present as biofilm on the gas-permeable membrane of the RWV chamber. We removed the biofilm from the membranes with silicon cell-scrapers and crystal violet stained the collected cells to assess total membrane attached biofilms. Under these RWV conditions, enhanced biofilm formation was readily apparent compared to the individual species (**Figure 5D**). Note that in the RWV system, *R. insidiosa* forms a more robust biofilm than in most other conditions reported in this study, reminiscent of its stronger biofilm on glass (**Figure 2A**).

<u>Testing potential mechanisms of biofilm enhancement</u>

Most of the previous descriptions of *R. insidiosa* stimulation of biofilm in mixed cultures showed that the effect was contact dependent and not co-aggregation based.

Our microscopy supported comingling of the two species (**Figure 2B**), but we also wanted to formally test whether a soluble factor or co-aggregation could explain the enhanced biofilm formation of this specific interaction. To test whether biofilm stimulation was transferrable by conditioned media, we used cell-free supernatants from *C. gleum*, *R. insidiosa*, or co-cultures mixed 1:1 with fresh media and measured biofilm formation in the flexible 96-well format. Neither single species nor the dual-species supernatants were able to stimulate biofilm formation (**Figure 6A**). This supports the direct interaction model but does not fully rule out potential for a soluble mediator, especially if the mediator is short-lived.

We assessed the potential for co-aggregation by mixing concentrated cultures of both species together and looking for any sedimentation caused by aggregation. At one hour there was no evidence of sedimentation (**Figure 6B**) and no sedimentation indicative of aggregation was apparent at times up to 24 h (data not shown).

Species and strain specificity for dual-species biofilm enhancement

Our primary goal was to characterize the interaction between the ISS *C. gleum* and *R. insidiosa* to understand our potable water model community. However, we also wanted to understand how broadly applicable this interaction was for other species in these genera and other strains of these species. We acquired non-ISS strains of *R. insidiosa*, *R. pickettii*, an unnamed *R. sp.*, *C. gleum*, *C. indologenes*, and *C. meningisepticum* (**Table 1**) and conducted biofilm assays in the flexible 96-well dish format. Most of the *R. insidiosa* strains could enhance ISS *C. gleum* biofilm formation, while only some of the other two Ralstonia species were able to do this (**Figure 7A, B**).

297 The ability of ISS *C. gleum* to respond to Ralstonia presence with enhanced biofilm
298 formation, however, was limited only to ISS *C. gleum* and very mild stimulation of *C.*
299 *meningisepticum* biofilm (**Figure 7A, C**). A big difference between the ISS *C. gleum* and
300 the other strains is that the other Chryseobacterium tested, particularly the *C. gleum*
301 strains, form robust biofilms on their own (**Figure 7A**).
302
303 **Discussion**
304 Here we examined the interaction between ISS-derived *R. insidiosa* and *C. gleum*
305 to better understand the enhanced biofilm of the dual-species cultures (**Figure 1**) as part
306 of community biofilm formation in our six-species potable water community [24]. The
307 enhanced biofilm formation between these two ISS strains is robust to starting inoculum
308 (**Figure 4**) and temperature (**Figure 5C**), does not occur in all growth media (**Figure 5B**),
309 and does not appear to be driven by a soluble mediator or co-aggregation (**Figure 6**).
310 While these findings shed light on the ISS *R. insidiosa* and *C. gleum* interaction, such
311 enhancement is not a common interaction outcome between these species based on our
312 examination of other *R. insidiosa* and *C. gleum* strains, as well as other species of
313 Ralstonia and Chryseobacterium (**Figure 7**). Thus, while the work presented here
314 increases our understanding of the potable water model system, we fully acknowledge
315 that most of the findings are not broadly extrapolatable to strains found outside of the ISS.
316 The enhanced biofilm formation between the ISS *R. insidiosa* and *C. gleum* is
317 readily apparent (**Figure 1A**) and is not driven by changes in total cell number or
318 proportional changes in cell number in the cultures (**Figure 1B**). The material presented
319 here is part of a broader characterization of the ISS potable water model community, and

thus has been underway for quite a number of years and with many different graduate, undergraduate, and technician contributors. It was during data examination for this report that we realized that there were two different MOPS media recipes co-existing in the lab differing only by their calcium concentrations. This calcium difference was sufficient to describe the higher biofilm formation by *C. gleum* monoculture observed by some lab members but not others (**Figure 3**). The general biofilm enhancement between the two ISS bacteria is still readily apparent at either calcium concentration, and the calcium concentration of the resultant MRLP media in each experiment is noted in each figure legend.

The enhancement of biofilm formation between the ISS *R. insidiosa* and *C. gleum* is very robust to starting inoculation (**Figure 4**). While we did not assess resulting CFUs for each species in these broader inoculation tests, we have no *a priori* reason to suspect that there are different mechanisms of enhancement at different starting inocula, though we cannot rule that out. The enhanced biofilm formation was seen at both 30ºC and 37ºC (**Figure 5C**) and occurred at room temperature (22-24ºC) in the RWV experiments (**Figure 5D**). The RWVs were used to ensure that the biofilm enhancement we observed in open, static biofilms was retained in a system mimicking the low shear environment found during growth in microgravity, as applicable to the ISS. While enhanced biofilm formation could happen with surprisingly low inoculum of *C. gleum*, no enhancement of biofilm could be seen in either direction by single culture or co-culture supernatants (**Figure 6A**), suggesting that there is either no soluble mediator or that any such mediator is very labile. Co-aggregation, while a common mechanism in biofilms particularly in the oral cavity, does not drive the enhanced biofilm formation in this interaction (**Figure 6B**).

When the ISS strains were grown in MRLP in the overnight cultures used for inoculation, there was observable dual-species biofilm enhancement in all tested media (**Figure 5A**), but when cells were instead grown in overnights of M9-RLP (**Figure 5B**) or M63-RLP (not shown) there was no biofilm enhancement in the subsequent M9-RLP or M63-RLP conditions, though enhancement was retained in MRLP and RL. We suspect that this is due to the relatively high phosphate concentration in the M9 and M63 media that could be suppressing biofilm enhancement. However, mechanistic dissection of the media component contribution to biofilm enhancement was halted once we determined that this interaction was not commonly shared between strains of these species (**Figure 7**).

The ISS *R. insidiosa* behaves similarly to most of the other *R. insidiosa* strains in terms of their weak monoculture biofilm formation and ability to enhance biofilm when grown with ISS *C. gleum* (**Figure 7**). Most of the *R. pickettii* strains do not show strong biofilm enhancement with *C. gleum*, nor does a *Ralstonia pickettii*-like species that has not yet been named. These similarities amongst the *R. insidiosa* strains suggest the ISS *R. insidiosa* and our mScarlet labeled derivative are potentially good representatives of the species. It is at least minimally genetically tractable, as we were able to generate an *attTn7*::*mScarlet* integrant that may be useful for studying *R. insidiosa* interaction studies with other bacteria.

The non-ISS *C. gleum* strains form strong biofilms, as shown in **Figure 7** and from literature reports [17], as do the two tested *C. indologenes* strains, while the two tested *C meningisepticum* strains do not. Thus, the ISS *C. gleum* appears to be non-representative of other *C. gleum* strains. While all our Chryseobacterium isolates tested were from

clinical sources, others in the literature were isolated from environmental sources and also show strong biofilm formation in monoculture. Thus, our ISS *C. gleum* appears only useful to describe its specific interactions amongst the ISS potable water bacteria.

In conclusion, we have presented partial dissection of an important interaction in a model potable water community. Despite the observations that this strain-specific interaction is unlikely to be broadly applicable beyond this model, we have provided additional information on basal biofilm formation amongst diverse *C. gleum* and *R. insidiosa* strains as well as generated an mScarlet-expressing *R. insidiosa* that may be useful to others in the field or studying *R. insidiosa* pathogenesis.

Conflicts of Interest

The authors declare that there are no conflicts of interest.

Funding Information

This study was supported by NASA cooperative agreements 20-EPSCoR2020-0079 and 16-EPSCoR2016-0019 to MJW. Graduate student rotation support for AF and BM was provided by the University of Vermont Cellular, Molecular, and Biomedical Sciences (CMB) Program. PD was supported by the Vermont Lung Center Multidisciplinary Training in Lung Biology T32 HL076122. ZZ was supported by a summer undergraduate research fellowship from the University of Vermont. Confocal microscopy was performed in the Microscopy Imaging Center at the University of Vermont on a Nikon

A1R-ER point scanning confocal, supported by NIH award number 1S10OD025030-01 from the Office of Research Infrastructure Programs. The funders had no role in study design, data collection and interpretation, or the decision to submit the work for publication.

Acknowledgements

We'd like to acknowledge the many undergraduate researchers and graduate rotation students who examined various aspects of the *R. insidiosa/C. gleum* interaction that are not reported here but still contributed holistically to our understanding of these two bacteria, including: Matthew Bompastore, Sierra Bruno, Brynn Cairns, Matthew Kinahan, Alexis Nadeau, Hannah Schulman, Alex Thompson, Sophie Unger, and Trevor Wolf.

Table 1: Description of strains used in this study

Strain#	Species	From	Source ID[a]	Source
Genus Ralstonia				
MJ602	*Ralstonia insidiosa*	ISS PW[b]	130770013-1	NASA JSC(cite)
MJ875	*Ralstonia insidiosa*	CF[c] sputum	AU13589	CFSS-UMich
MJ880	*Ralstonia insidiosa*	CF sputum	AU16942	CFSS-UMich
MJ885	*Ralstonia insidiosa*	Liver biopsy	AU19393	CFSS-UMich
MJ886	*Ralstonia insidiosa*	CF sputum	AU20290	CFSS-UMich
MJ890	*Ralstonia insidiosa*	CF sputum	AU20795	CFSS-UMich
MJ891	*Ralstonia insidiosa*	CF sputum	AU21215	CFSS-UMich
MJ899	*Ralstonia insidiosa*	CF sputum	AU2944	CFSS-UMich
MJ912	*Ralstonia insidiosa*	CF sputum	AU37532	CFSS-UMich
MJ913	*Ralstonia insidiosa*	CF sputum	AU40266	CFSS-UMich
MJ915	*Ralstonia insidiosa*	CF sputum	AU42598	CFSS-UMich
MJ916	*Ralstonia insidiosa*	Blood	AU5199	CFSS-UMich
MJ918	*Ralstonia insidiosa*	CF sputum	AU9058	CFSS-UMich
MJ919	*Ralstonia insidiosa*	CF sputum	AU9775	CFSS-UMich
MJ926	*Ralstonia insidiosa*	Water	HI4151	CFSS-UMich
MJ873	*Ralstonia pickettii*	Dialysis fluid	AU10444	CFSS-UMich
MJ876	*Ralstonia pickettii*	CF sputum	AU14824	CFSS-UMich
MJ877	*Ralstonia pickettii*	Deep wound	AU15492	CFSS-UMich
MJ882	*Ralstonia pickettii*	CF sputum	AU17622	CFSS-UMich
MJ884	*Ralstonia pickettii*	CF sputum	AU17695	CFSS-UMich
MJ887	*Ralstonia pickettii*	CF sputum	AU20306	CFSS-UMich
MJ892	*Ralstonia pickettii*	Blood	AU21292	CFSS-UMich
MJ895	*Ralstonia pickettii*	CF sputum	AU27711	CFSS-UMich
MJ897	*Ralstonia pickettii*	CF swab	AU28427	CFSS-UMich
MJ898	*Ralstonia pickettii*	CF sputum	AU28504	CFSS-UMich
MJ900	*Ralstonia pickettii*	CF throat	AU30485	CFSS-UMich
MJ911	*Ralstonia pickettii*	CF sputum	AU36159	CFSS-UMich
MJ914	*Ralstonia pickettii*	CF ET[d] aspirate	AU40593	CFSS-UMich

MJ917	*Ralstonia pickettii*	Pericardium	AU6150	CFSS-UMich
MJ920	*Ralstonia pickettii*	Soil	HI2644	CFSS-UMich
MJ921	*Ralstonia pickettii*	IV^{e} saline	HI2937	CFSS-UMich
MJ922	*Ralstonia pickettii*	Environmental	HI3561	CFSS-UMich
MJ923	*Ralstonia pickettii*	Environmental	HI3575	CFSS-UMich
MJ924	*Ralstonia pickettii*	Environmental	HI3597	CFSS-UMich
MJ925	*Ralstonia pickettii*	Environmental	HI3631	CFSS-UMich
MJ874	*Ralstonia* sp. 1	CF sputum	AU11313	CFSS-UMich
MJ879	*Ralstonia* sp. 2	Blood	AU15928	CFSS-UMich
MJ881	*Ralstonia* sp. 2	ET aspirate	AU17267	CFSS-UMich
MJ883	*Ralstonia* sp. 2	CF sputum	AU17666	CFSS-UMich

Genus Chryseobacterium

MJ601	*Chryseobacterium gleum*	ISS PW	113330055-2	NASA JSC(cite)
MJ878	*Chryseobacterium gleum*	CF sputum	AU15601	CFSS-UMich
MJ893	*Chryseobacterium gleum*	CF sputum	AU23904	CFSS-UMich
MJ894	*Chryseobacterium gleum*	CF throat	AU25398	CFSS-UMich
MJ896	*Chryseobacterium gleum*	CF sputum	AU28136	CFSS-UMich
MJ901	*Chryseobacterium gleum*	CF sputum	AU32207	CFSS-UMich
MJ902	*Chryseobacterium gleum*	CF nasopharynx	AU32450	CFSS-UMich
MJ903	*Chryseobacterium gleum*	CF throat	AU33652	CFSS-UMich
MJ904	*Chryseobacterium gleum*	CF sputum	AU33758	CFSS-UMich
MJ905	*Chryseobacterium gleum*	CF nasopharynx	AU34337	CFSS-UMich
MJ907	*Chryseobacterium gleum*	CF sputum	AU34937	CFSS-UMich
MJ908	*Chryseobacterium gleum*	CF	AU35407	CFSS-UMich
MJ910	*Chryseobacterium gleum*	CF sputum	AU36080	CFSS-UMich
MJ906	*Chryseobacterium indologenes*	CF throat	AU34532	CFSS-UMich
MJ909	*Chryseobacterium indologenes*	CF sputum	AU35927	CFSS-UMich
MJ888	*Chryseobacterium meningisepticum*	CF sputum	AU20341	CFSS-UMich
MJ889	*Chryseobacterium meningisepticum*	CF sputum	AU20342	CFSS-UMich

463 a- The database ID at the source repository

464 b- PW, potable water

465 c- Sputum from a person with cystic fibrosis (CF)

466 d- ET, endotracheal

467 e- IV, intravenous

468

REFERENCES

1. Castro VA, Thrasher AN, Healy M, Ott CM, Pierson DL. Microbial characterization during the early habitation of the International Space Station. Microb Ecol. 2004;47(2):119-26; doi: 10.1007/s00248-003-1030-y.
2. Cardinale M, Kaiser D, Lueders T, Schnell S, Egert M. Microbiome analysis and confocal microscopy of used kitchen sponges reveal massive colonization by Acinetobacter, Moraxella and Chryseobacterium species. Sci Rep. 2017;7(1):5791; doi: 10.1038/s41598-017-06055-9.
3. Hong PY, Hwang C, Ling F, Andersen GL, LeChevallier MW, Liu WT. Pyrosequencing analysis of bacterial biofilm communities in water meters of a drinking water distribution system. Appl Environ Microbiol. 2010;76(16):5631-5; doi: 10.1128/AEM.00281-10.
4. Ling F, Whitaker R, LeChevallier MW, Liu WT. Drinking water microbiome assembly induced by water stagnation. ISME J. 2018;12(6):1520-31; doi: 10.1038/s41396-018-0101-5.
5. Dias MF, da Rocha Fernandes G, Cristina de Paiva M, Christina de Matos Salim A, Santos AB, Amaral Nascimento AM. Exploring the resistome, virulome and microbiome of drinking water in environmental and clinical settings. Water Res. 2020;174:115630; doi: 10.1016/j.watres.2020.115630.
6. Perrin Y, Bouchon D, Delafont V, Moulin L, Hechard Y. Microbiome of drinking water: A full-scale spatio-temporal study to monitor water quality in the Paris distribution system. Water Res. 2019;149:375-85; doi: 10.1016/j.watres.2018.11.013.
7. Szewzyk U, Szewzyk R, Manz W, Schleifer KH. Microbiological safety of drinking water. Annu Rev Microbiol. 2000;54:81-127; doi: 10.1146/annurev.micro.54.1.81.
8. Vaz-Moreira I, Nunes OC, Manaia CM. Ubiquitous and persistent Proteobacteria and other Gram-negative bacteria in drinking water. Sci Total Environ. 2017;586:1141-9; doi: 10.1016/j.scitotenv.2017.02.104.
9. Ryan MP, Adley CC. The antibiotic susceptibility of water-based bacteria Ralstonia pickettii and Ralstonia insidiosa. J Med Microbiol. 2013;62(Pt 7):1025-31; doi: 10.1099/jmm.0.054759-0.
10. Lee J, Lee CS, Hugunin KM, Maute CJ, Dysko RC. Bacteria from drinking water supply and their fate in gastrointestinal tracts of germ-free mice: a phylogenetic comparison study. Water Res. 2010;44(17):5050-8; doi: 10.1016/j.watres.2010.07.027.
11. Coenye T, Goris J, De Vos P, Vandamme P, LiPuma JJ. Classification of Ralstonia pickettii-like isolates from the environment and clinical samples as Ralstonia insidiosa sp. nov. Int J Syst Evol Microbiol. 2003;53(Pt 4):1075-80; doi: 10.1099/ijs.0.02555-0.
12. Fluit AC, Bayjanov JR, Aguilar MD, Canton R, Tunney MM, Elborn JS, et al. Characterization of clinical Ralstonia strains and their taxonomic position. Antonie Van Leeuwenhoek. 2021;114(10):1721-33; doi: 10.1007/s10482-021-01637-0.

13. Fang Q, Feng Y, Feng P, Wang X, Zong Z. Nosocomial bloodstream infection and the emerging carbapenem-resistant pathogen Ralstonia insidiosa. BMC Infect Dis. 2019;19(1):334; doi: 10.1186/s12879-019-3985-4.
14. Ryan MP, Adley CC. Ralstonia spp.: emerging global opportunistic pathogens. Eur J Clin Microbiol Infect Dis. 2014;33(3):291-304; doi: 10.1007/s10096-013-1975-9.
15. Chiu CW, Li MC, Ko WC, Li CW, Chen PL, Chang CM, et al. Clinical impact of Gram-negative nonfermenters on adults with community-onset bacteremia in the emergency department. J Microbiol Immunol Infect. 2015;48(1):92-100; doi: 10.1016/j.jmii.2013.08.004.
16. Tsouvalas CP, Mousa G, Lee AH, Philip JA, Levine D. Chryseobacterium gleum Isolation from Respiratory Culture Following Community-Acquired Pneumonia. Am J Case Rep. 2020;21:e921172; doi: 10.12659/AJCR.921172.
17. Lo HH, Chang SM. Identification, characterization, and biofilm formation of clinical Chryseobacterium gleum isolates. Diagn Microbiol Infect Dis. 2014;79(3):298-302; doi: 10.1016/j.diagmicrobio.2014.01.027.
18. Guo A, Xu Y, Mowery J, Nagy A, Bauchan G, Nou XW. Ralstonia insidiossa induces cell aggregation of Listeria monocytogenes. Food Control. 2016;67:303-9.
19. Liu NT, Nou XW, Lefcourt AM, Shelton DR, Lo YM. Dual-species biofilm formation by Escherichia coli O157:H7 and environmental bacteria isolated from fresh-cut processing facilities. International Journal of Food Microbiology. 2014;171:15-20; doi: 10.1016/j.ijfoodmicro.2013.11.007.
20. Liu NT, Nou XW, Bauchan GR, Murphy C, Lefcourt AM, Shelton DR, et al. Effects of Environmental Parameters on the Dual-Species Biofilms Formed by Escherichia coli O157:H7 and Ralstonia insidiosa, a Strong Biofilm Producer Isolated from a Fresh-Cut Produce Processing Plant. Journal of Food Protection. 2015;78(1):121-7; doi: 10.4315/0362-028x.Jfp-14-302.
21. Liu NT, Bauchan GR, Francoeur CB, Shelton DR, Lo YM, Nou XW. Ralstonia insidiosa serves as bridges in biofilm formation by foodborne pathogens Listeria monocytogenes, Salmonella enterica, and Enterohemorrhagic Escherichia coli. Food Control. 2016;65:14-20; doi: 10.1016/j.foodcont.2016.01.004.
22. Xu Y, Nagy A, Bauchan GR, Xia X, Nou X. Enhanced biofilm formation in dual-species culture of Listeria monocytogenes and Ralstonia insidiosa. AIMS Microbiol. 2017;3(4):774-83; doi: 10.3934/microbiol.2017.4.774.
23. Roder HL, Raghupathi PK, Herschend J, Brejnrod A, Knochel S, Sorensen SJ, et al. Interspecies interactions result in enhanced biofilm formation by co-cultures of bacteria isolated from a food processing environment. Food Microbiol. 2015;51:18-24; doi: 10.1016/j.fm.2015.04.008.
24. Thompson AF, English EL, Nock AM, Willsey GG, Eckstrom K, Cairns B, et al. Characterizing species interactions that contribute to biofilm formation in a multispecies model of a potable water bacterial community. Microbiology (Reading). 2020;166(1):34-43; doi: 10.1099/mic.0.000849.
25. Labauve AE, Wargo MJ. Growth and Laboratory Maintenance of Pseudomonas aeruginosa. Curr Protoc Microbiol. 2012;Chapter 6:Unit6E 1; doi: 10.1002/9780471729259.mc06e01s25.

559 26. Merritt JH, Kadori DE, O'Toole GA. Growing and Analyzing Static Biofilms. In:
560 Current Protocols in Microbiology. Hoboken, NJ: J. Wiley & Sons; 2005. p. 1-17.
561 27. Schlechter RO, Jun H, Bernach M, Oso S, Boyd E, Munoz-Lintz DA, et al.
562 Chromatic Bacteria - A Broad Host-Range Plasmid and Chromosomal Insertion
563 Toolbox for Fluorescent Protein Expression in Bacteria. Front Microbiol.
564 2018;9:3052; doi: 10.3389/fmicb.2018.03052.
565

566

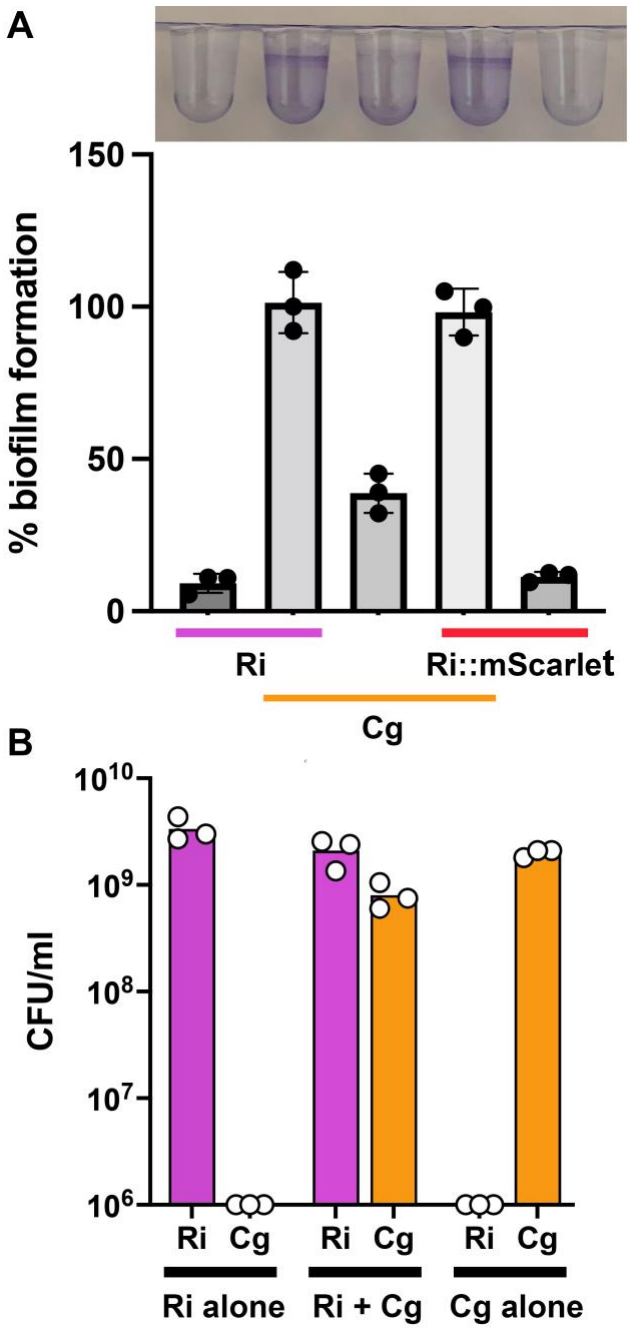

567

568 **Figure 1. Enhanced biofilm formation during *Ralstonia insidiosa* and**
569 ***Chryseobacterium gleum* coculture.** The ISS isolates of *R. insidiosa* (Ri) and *C. gleum*
570 (Cg) grown alone or cocultured in high-calcium MRLP medium for 24 hours. (**A**) (Top)
571 Representative crystal violet stain of these static biofilms grown in flexible 96-well dishes,
572 with samples in the same order as the graph. (Bottom) Quantification of the crystal violet
573 biofilm absorbance normalized to *R. insidiosa*+*C. gleum* as 100% biofilm formation.
574 Integration of *mScarlet* at the *attTn7* site (Ri::mScarlet) does not impact *R. insidiosa*'s

biofilm formation or interaction with *C. gleum*. **(B)** Quantification of planktonic and biofilm cells from the mono- or co-culture wells. After scraping, vortexing, and resuspension, colony forming units were counted by serial dilution plating and subsequent counting. The y-axis starts at 10^6 CFU as that was the detection limit for these dilutions. For each panel, each individual dot is the mean of three technical replicates on a separate experimental day. For (A), using ANOVA with a Sidak's post-test, the biofilm formed by the co-cultures was significantly higher than that formed by the respective monocultures ($p < 0.001$) and was also significantly higher than the sum of the monoculture biofilms ($p < 0.005$). For (B), using a two-way ANOVA with Tukey's post-test, the co-culture does not significantly impact the CFU of the individual bacteria compared to monoculture and the total cells per well are also not significantly altered.

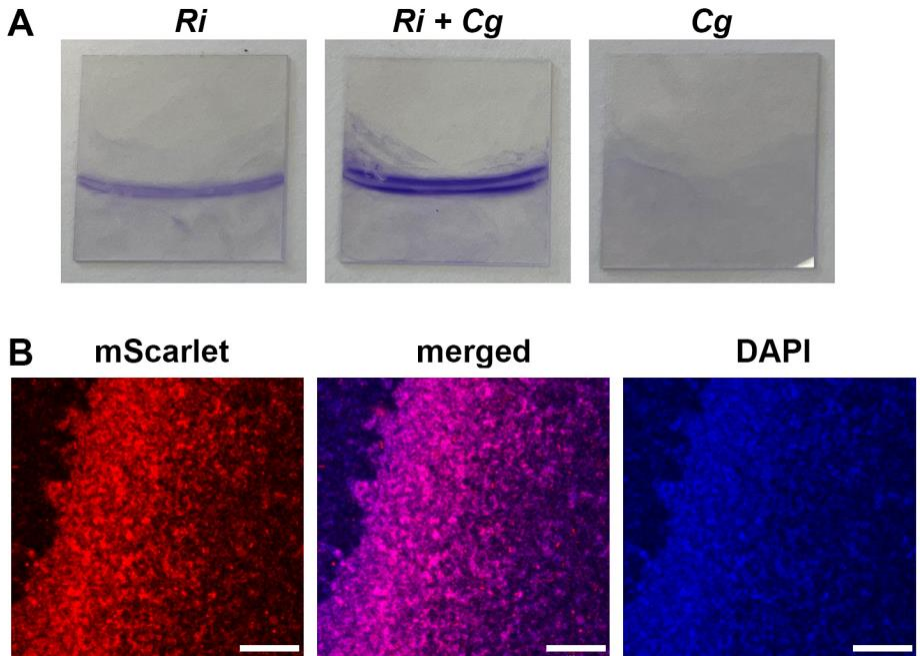

Figure 2. **Enhanced dual-species biofilm formation on glass coverslips by *C. gleum* and *R. insidiosa attTn7*::mScarlet.** The ISS isolates *C. gleum* (Cg) and the mScarlet-expressing *R. insidiosa* (*Ri*) were grown alone or cocultured in high-calcium MRLP medium for 24 hours in 12-well plates with a vertically oriented coverslip in each well. **(A)** Crystal violet staining of the coverslip biofilm. Note that *R. insidiosa* forms more biofilm on glass than on plastic (Figure 1). **(B)** One example Z-section of the dual-species biofilm taken approximately 3 µm above the coverslip using confocal microscopy. The air-liquid interface runs roughly diagonally on a line rotated slightly clockwise from vertical with the air side on the left. Scale bar = 100 µm.

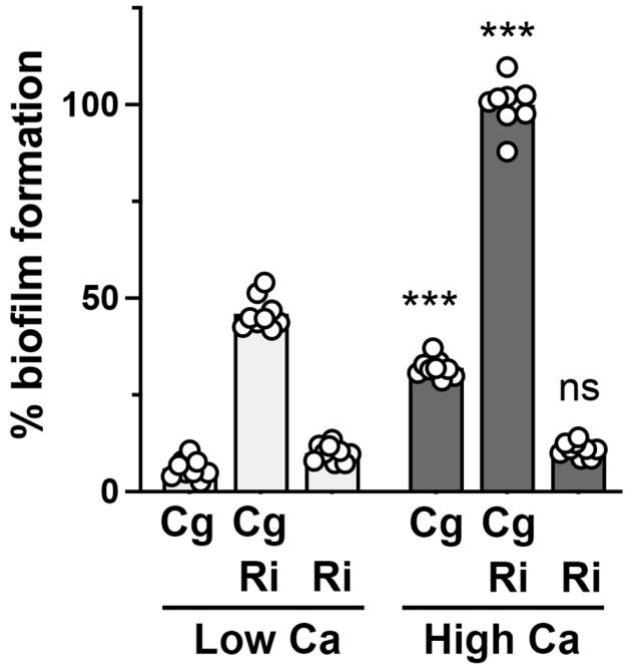

Figure 3. **Impact of calcium on biofilm formation by *C. gleum.*** More biofilm is generated by *C. gleum* and the dual species biofilm when grown in high calcium (400 µM) MOPS media versus low calcium (21.1 µM) MOPS media. Calcium concentration did not impact *R. insidiosa* biofilm formation. Dots represent individual experimental replicates from three independent experiments; statistic calculated using the means of each experiment. Two-way ANOVA with a Sidak's multiple comparison test separately comparing each species composition between the two calcium conditions. ***, $p < 0.001$; ns, not significant.

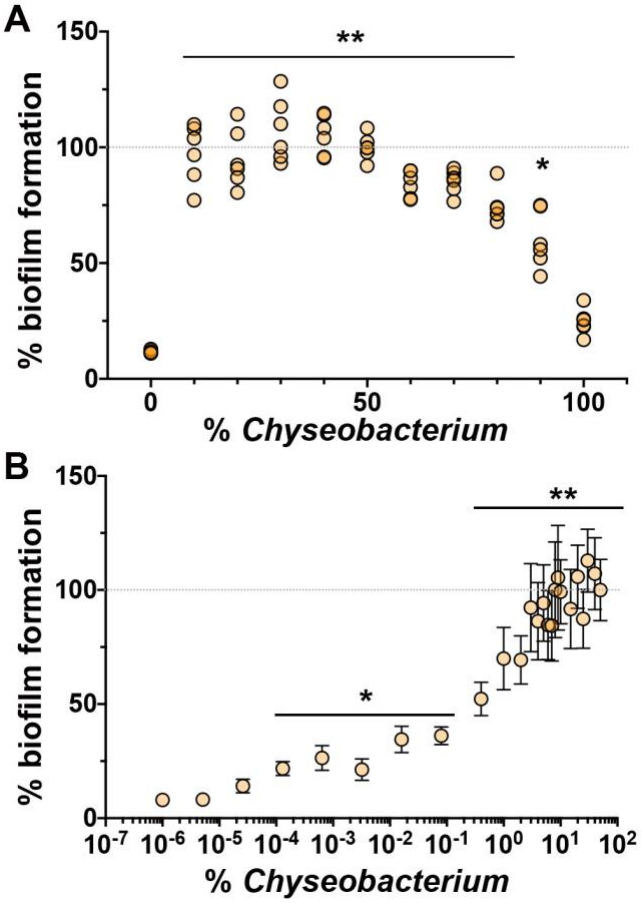

Figure 4. Biofilm stimulation with varying initial concentrations of *C. gleum*. The ISS *C. gleum* was added as a percentage of the initial starting OD_{600} noted on the x-axis with the remainder being comprised of ISS *R. insidiosa*. All experiments conducted in high calcium MOPS **(A)** *C. gleum* stimulation of dual-species biofilm formation decreases as the *C. gleum* composition increases above 50% but shows stable stimulation as *C. gleum* composition drops below 50%. Each dot represents the measurement of a biological replicate from three separate experiments (two replicates per experiment). **(B)** Dilution to extinction of *C. gleum* shows biofilm stimulation above *R. insidiosa* alone (the zero *C. gleum* condition is set as the 10^{-6} dot), showing that biofilm stimulation can be seen with as little as 0.0001% *C. gleum*. Dots represent the mean of at least three independent experiments and the error bars represent standard deviation. The grey dotted line marks the 100% biofilm formation that is set based on the 50/50 *R. insidiosa*, *C. gleum* mix and all other biofilm formation is normalized to this 100% mark. Data were analyzed with Browne-Forsythe and Welch ANOVA with a Dunnett's post-test with 100% *C. gleum* as the comparator in (A) and 100% *R. insidiosa* as the comparator in (B). *, $p < 0.05$; **, $p < 0.01$.

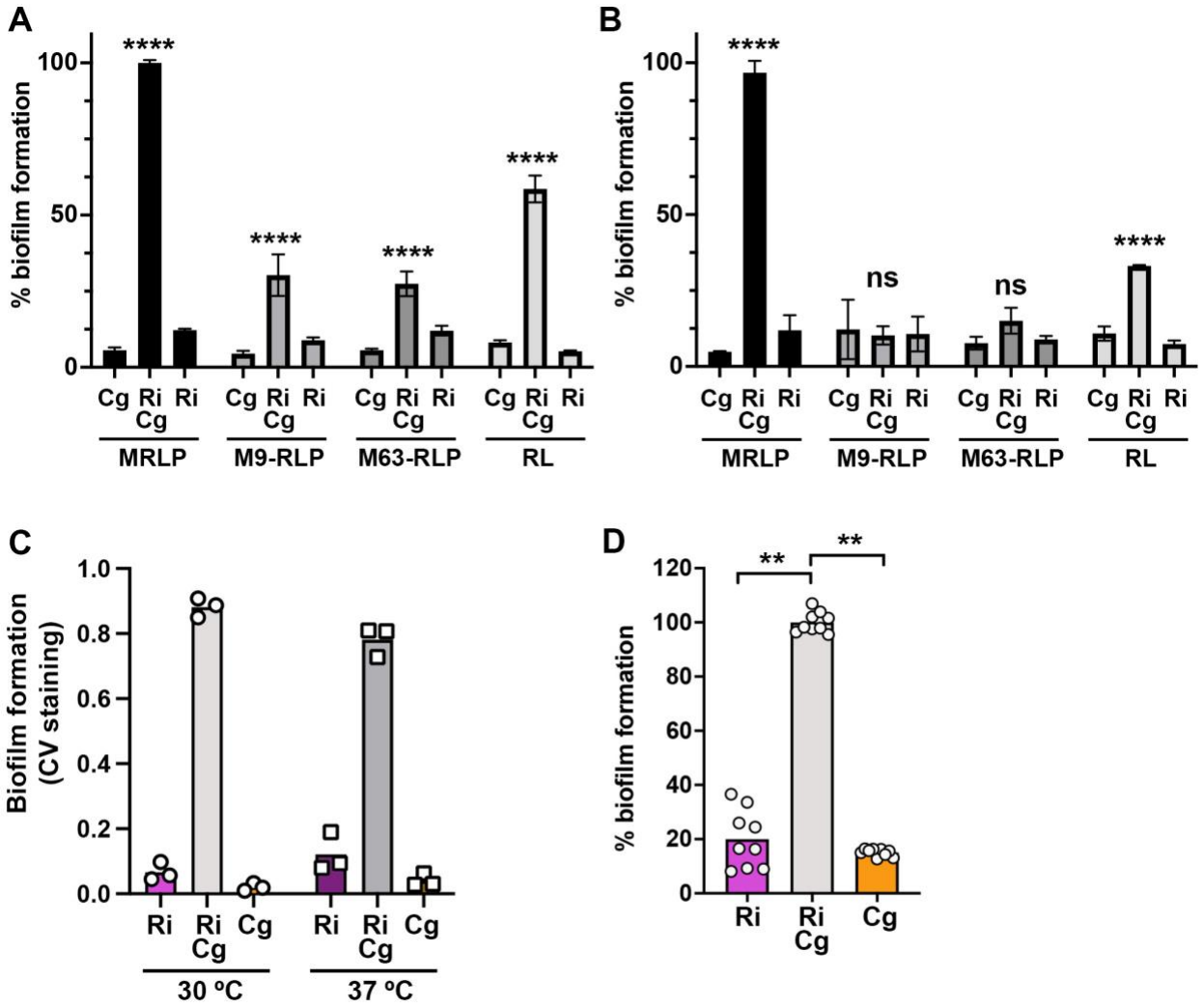

Figure 5. Characterization of growth media, temperature, and low-shear growth on enhanced biofilm formation. **(A)** Biofilm formation normalized to Ri+Cg MRLP for the media listed below the x-axis, with cells pre-grown in low calcium MRLP. **(B)** Normalized biofilm formation in the media listed below the x-axis, with cells pre-grown in low calcium M9-RLP. Data in (B) is normalized to Ri+Cg in MRLP from (A). Means from three independent experimental days, error bars represent standard deviation. **(C)** Biofilm formation from the noted single or dual-species cultures in low calcium MRLP grown at 30ºC (left), or 37ºC (right). Each point represents the mean of three biological replicates for each of three independent experimental days. **(D)** Biofilm formation on the gas-permeable membrane of a rotating wall vessel (RWV) in high calcium MRLP. Each point represents each replicate of the RWV experiment, though statistics calculated from each experimental day's mean (i.e. n=3). Statistics for (A,B,C) done using 2-way ANOVA with a Dunnett's corrected multiple comparison post-test comparing each single species biofilm to the dual-species biofilm within each media or condition. Statistic for (D) using Welch's ANOVA with Dunnett's post-test comparing each single species biofilm to the dual-species biofilm.

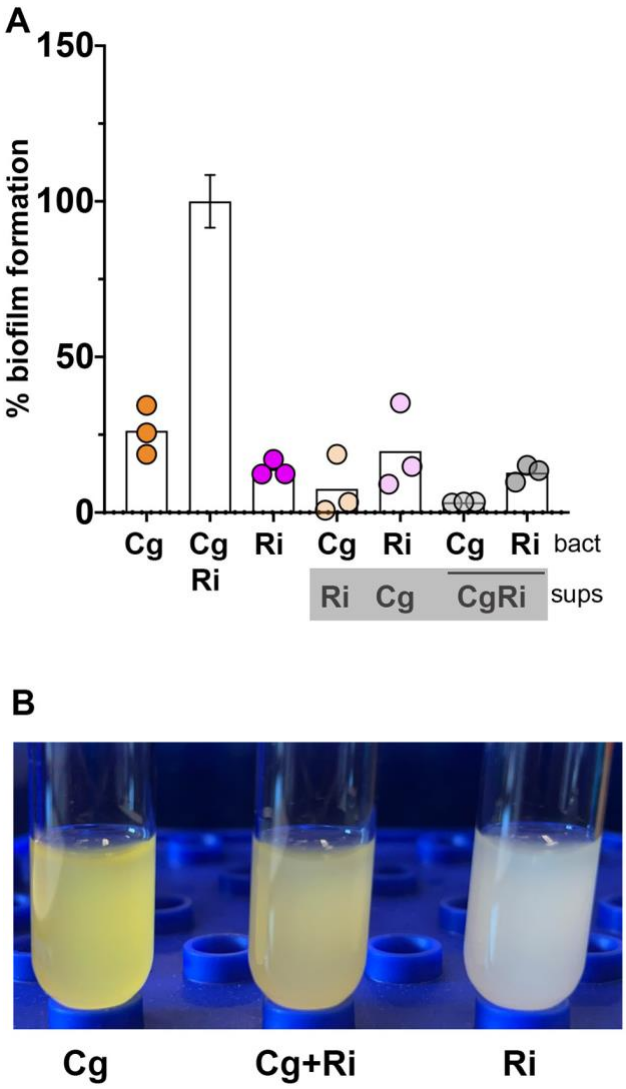

Figure 6. The biofilm enhancing effect of either species cannot be transferred by supernatant and is not due to co-aggregation. **(A)** The enhancement in biofilm formation seen in the dual-species growth is not conferred by cell-free supernatant from either the single or dual-species conditions using 50% spent supernatant and 50% fresh media. None of the supernatant treatments were significantly different than their single species growth after correction for multiple comparisons using a Brown-Forsythe and Welch ANOVA with a Dunnett's post-test comparing all means to each other. The source of the supernatants tested is present in the grey box under the species abbreviation. Each dot represents the mean from three biological replicates per experiment. The Cg/Ri conditions is set to 100% for each experiment to normalize between experiments, so the average standard deviation for 50/50 Cg-Ri mixes is displayed. **(B)** There is no co-aggregation apparent between these strains. Cells grown in the high-Ca MOPS media were collected by centrifugation and resuspended at a final concentration of OD600 = 6 and examined over time with the picture representative of all replicates at one hour post mixing.

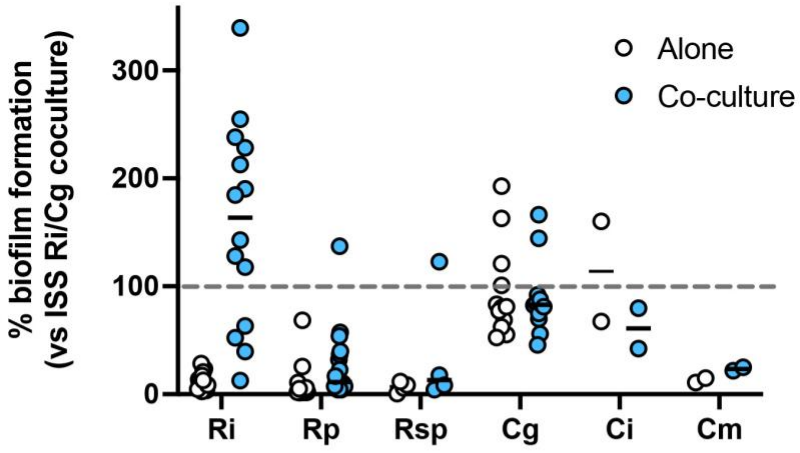

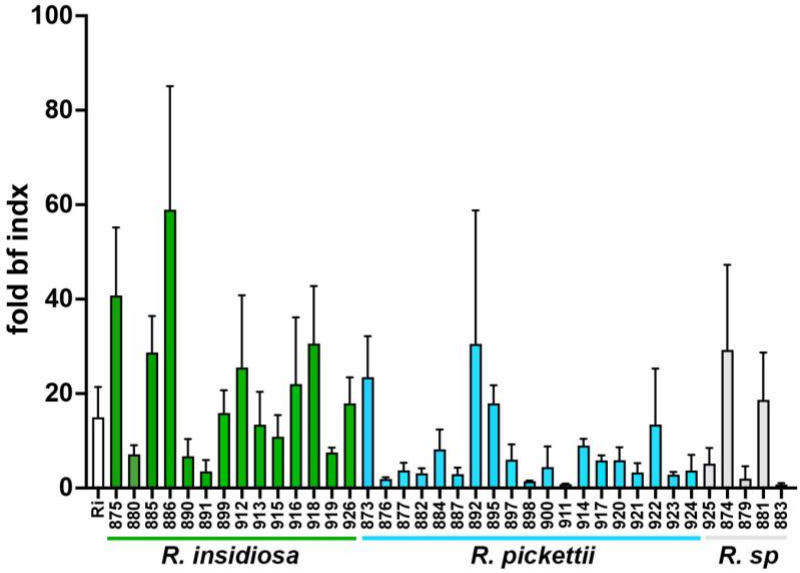

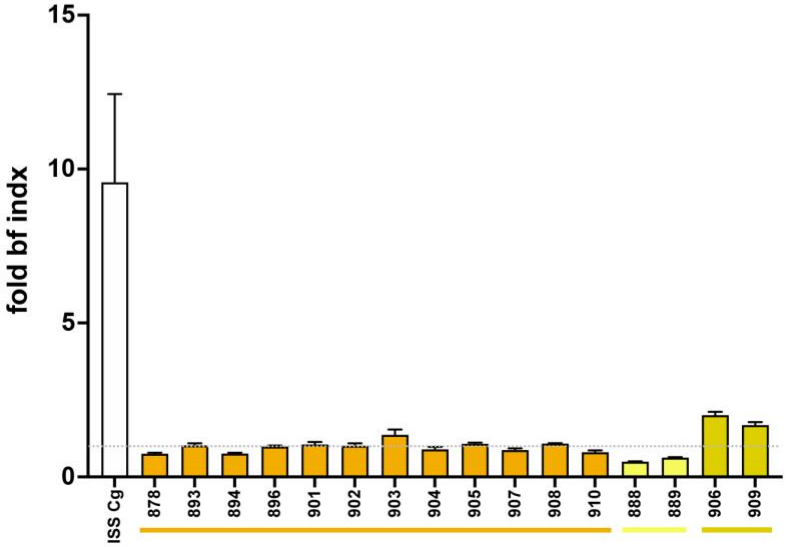

Figure 7. Strain and species specificity for dual-species biofilm enhancement. **(A)** Biofilm quantification normalized by setting the intraday ISS *R. insidiosa* and ISS *C. gleum* dual-species biofilm as 100% biofilm formation. White circles are data for each species alone and the blue circles are in the presence of either the ISS *C. gleum* (for Ralstonia species) or the ISS *R. insidiosa* (for the Chryseobacterium species). Two-way repeated measures ANOVA with Sidak's multiple comparison test comparing intra-species mono- and dual-species biofilms supports that at the species level, only *R. insidiosa* shows significant biofilm enhancement under dual species conditions ($p < 0.001$). **(B)** The same data contributing to panel (A) converted to fold change of dual species biofilm divided by biofilm formation by that strain alone. Green bars are the *R. insidiosa* strains, blue are *R. pickettii* strains, and grey are an unnamed Ralstonia species. **(C)** The same data contributing to panel (A) represented as fold change of dual species biofilm divided by biofilm formation by that strain alone. The white bar is the ISS *C. gleum*, orange bars are the non-ISS *C. gleum* strains, yellow are *C. indologenes* strains, and mustard are *C. meningisepticum* strains.